Pergamon

Int. J. Solids Structures Vol. 35, Nos 34–35, pp. 4845–4867, 1998

Printed in Great Britain
0020-7683/98/$—see front matter

PII: S0020-7683(98)00097-3

CONSOLIDATION OF A DOUBLE-POROSITY MEDIUM

K. T. LEWALLEN† and H. F. WANG
Department of Geology and Geophysics, University of Wisconsin-Madison, U.S.A.

(*Received* 21 *April* 1997; *in revised form* 18 *December* 1997)

Abstract—The classical one-dimensional column consolidation boundary value problem is studied for a double-porosity material. Uniaxial strain and constant vertical stress conditions are applied to a column that is drained at the top and undrained at the bottom. An initial fluid pressure differential develops between the matrix and fracture phases in response to surface loading when variations in the mechanical and flow parameters of the matrix and fracture exist. The mean stress is shown to be a linear combination of the fluid pressure in the matrix and the fluid pressure in the fracture. The time dependent general analytical solution is given for the matrix and fracture pressure histories and surface displacements using fracture and matrix storage coefficients defined for constant stress (constant confining pressure) and the assumption that the cross-storage coefficient at constant stress is negligible. Pressure and displacement histories are controlled by the mechanical and flow properties of both the matrix and fracture and on the magnitude of the differences between the two phases. The double-porosity solution approaches the equivalent single porosity solution for closely spaced fractures, a small permeability contrast and a large cross-flow term. Pressures and displacements are also compared to previous results in the literature based on storage coefficients defined at constant volumetric strain and the assumption that the constant strain cross-storage coefficient is negligible. The previous results included small matrix fluid pressures and fracture fluid pressures in excess of the applied stress. The constant stress formulation of the double-porosity column consolidation problem produces physically intuitive results.

NOMENCLATURE

a_{ij}	stress-based poroelastic coefficients
A_{ij}	strain-based poroelastic coefficients
$B^{(1)}$, $B^{(2)}$	Skempton's coefficient for the matrix, fracture
G	shear modulus
h	total column height
k	combined matrix–fracture system permeability
k_1, k_2	permeability of the matrix, fracture
K	combined matrix–fracture system bulk modulus
K_f	pore fluid bulk modulus
K_s	unjacketed bulk modulus for the composite frame
$K_v^{(d)}$	drained vertical bulk modulus
$K_v^{(u)}$	undrained vertical bulk modulus
L	fracture spacing
p_c	confining pressure
$p_f^{(1)}$, $p_f^{(2)}$	fluid pressure in the matrix, fracture
$p_u^{(1)}$, $p_u^{(2)}$	undrained pore fluid pressure in the matrix, fracture
S	combined matrix–fracture system storage coefficient
S_1, S_2	storage coefficient of the matrix, fracture
s_n	fracture normal stiffness
s_s	fracture shear stiffness
t	time
t_D	dimensionless time
U	displacement
U_c	displacement due to consolidation
$U^{(d)}$, $U^{(u)}$	displacement for drained conditions, undrained conditions
U_T	total displacement
x	distance below the column's top boundary
α	Biot–Willis parameter $(1 - K/K_s)$
ε	volumetric strain (positive in expansion)

† Author to whom correspondence should be addressed. Exxon Exploration Co., P.O. Box 4778, Houston, TX 77210-4778, U.S.A. Tel.: 001 281 423 7546. E-mail: badger—Tex@msn.com

$\gamma^{(1)}, \gamma^{(2)}$	loading efficiency for the matrix, fracture
κ	cross-flow constant of proportionality
μ	fluid viscosity
ν	Poisson's ratio
ϕ	porosity
σ	stress
$\zeta^{(1)}, \zeta^{(2)}$	increment of fluid content in the matrix, fracture (positive for a net gain of fluid)

INTRODUCTION

The response of many Earth materials can be adequately approximated using a linear elastic theory. The presence of fluid in a porous medium requires additional terms in the elastic equations to account for the coupling between the mechanical behavior of the rock mass and fluid flow. For example, pore pressures rise in response to compression of the medium if the compression is fast relative to fluid flow. An increase in pore pressure, on the other hand, induces a dilation of the rock mass. This coupled fluid flow-deformation behavior, poroelasticity, was first studied by Terzaghi (1923) as a one-dimensional soil consolidation problem for a homogeneous, porous medium.

Naturally fractured rock formations form important subsurface flow systems with a high degree of local heterogeneity. Fracture flow velocities can be high compared to movement through the interconnected pore spaces in the matrix. Dominant fluid storage occurs in the matrix blocks. Aquifer or reservoir systems which contain both open fractures and interconnected pore spaces are often modeled as a double-porosity medium (Barenblatt *et al.*, 1960; Warren and Root, 1963).

The poroelastic behavior of double-porosity rocks depends on both the flow and mechanical parameters of the fracture as well as the matrix. The coupling between the mechanical behavior and fluid dynamics in double-porosity rocks must be understood in order to predict reservoir or aquifer performance. Storage coefficient is one property that describes the coupling. Biot (1941) described the coupling between the fluid pressure and stress fields using linear elastic theory for a homogeneous, porous medium. Several authors (Wilson and Aifantis, 1982; Khaled *et al.*, 1984; Beskos and Aifantis, 1986; Elsworth and Bai, 1990, 1992; Bai *et al.*, 1993) have extended the linear formulation to identify the elastic coefficients of double-porosity models in a strain-based formulation. Berryman and Wang (1995) presented an alternative set of constitutive equations using a stress-based formulation. Tuncay and Corapcioglu (1995) derived an effective stress principle for a double-porosity medium using volume averaging techniques and obtained identical results to Berryman and Wang (Wang and Berryman, 1996).

Specifically, the purpose of this investigation is to use the stress-based constitutive theory of Berryman and Wang (1995) to recalculate solutions to the classical one-dimensional column consolidation boundary value problem using measured double-porosity rock parameters. The governing equations and assumptions are reviewed. An analytical solution is derived for the stress-based formulation. Numerical results are examined to observe the linear coupling between deformation and fluid flow. The solutions are compared to previously published results, which were calculated using different assumptions. Insight is gained concerning the flow characteristics and storage capacity in double-porosity media as influenced by the imposed stress fields.

CONSTITUTIVE EQUATIONS

Static constitutive equations have been formulated by extending Biot's concepts of poroelasticity to double-porosity rocks. It is assumed that the double-porosity sample under investigation has been selected at an appropriate size such that the composite rock/pore/fracture/fluid mixture is both homogeneous and isotropic. Two equivalent formulations exist. The difference between the formulations is the selection of the independent vs dependent variables in the constitutive equations. Wilson and Aifantis (1982) selected volumetric strain (positive in expansion), ε, matrix fluid pressure, $p_f^{(1)}$, and fracture fluid pressure, $p_f^{(2)}$, as independent variables. The dependent variables are external confining

pressure, p_c, and increment of fluid content (fluid volume accumulation per unit bulk volume) in the matrix, $\zeta^{(1)}$, and fracture, $\zeta^{(2)}$ (positive for a net gain in fluid in the control volume). The storage coefficients, which are identified and discussed later, are defined at constant total strain. Linear relations among the variables for this strain-based formulation take the general form

$$\begin{pmatrix} -\delta p_c \\ -\delta\zeta^{(1)} \\ -\delta\zeta^{(2)} \end{pmatrix} = \begin{pmatrix} A_{11} & A_{12} & A_{13} \\ A_{21} & A_{22} & A_{23} \\ A_{31} & A_{32} & A_{33} \end{pmatrix} \begin{pmatrix} \delta\varepsilon \\ -\delta p_f^{(1)} \\ -\delta p_f^{(2)} \end{pmatrix}. \tag{1}$$

Alternatively, Berryman and Wang (1995) exchanged the roles of confining pressure and volumetric strain. The storage coefficients are defined in terms of constant confining pressure or constant stress. The constitutive equations in the stress-based formulation have the matrix form

$$\begin{pmatrix} \delta\varepsilon \\ -\delta\zeta^{(1)} \\ -\delta\zeta^{(2)} \end{pmatrix} = \begin{pmatrix} a_{11} & a_{12} & a_{13} \\ a_{21} & a_{22} & a_{23} \\ a_{31} & a_{32} & a_{33} \end{pmatrix} \begin{pmatrix} -\delta p_c \\ -\delta p_f^{(1)} \\ -\delta p_f^{(2)} \end{pmatrix}. \tag{2}$$

This double-porosity, stress-based formulation has a symmetric coefficient matrix with six independent poroelastic coefficients for isotropic stress. For comparison, a single-porosity material under isotropic stress has just three independent poroelastic coefficients. The six coefficients for double-porosity rocks occur in three categories that correspond to the three original Biot coefficients. The coefficient $a_{11} = 1/K$ is the compressibility of the combined fracture-matrix system. The coefficients a_{12} and a_{13} are the generalized poroelastic expansion coefficients of the matrix and fracture, respectively. The terms a_{22}, a_{23}, a_{33} are generalized storage coefficients: a_{22} is the storage coefficient of the matrix, a_{33} represents storage in the fracture, a_{23} is the cross-storage term.

A complete description of the relationship between the independent and dependent parameters is obtained by determining the six independent coefficients. Four combinations of these coefficients are established directly from laboratory measurements. A fifth condition is obtained by requiring the overall compressibility to be the volume average of the matrix compressibility and fracture compressibility. The sixth condition requires an assumption concerning the coupling between the matrix and fracture.

The cross-storage coefficient is defined as

$$a_{23} = \left.\frac{\delta\zeta^{(1)}}{\delta p_f^{(2)}}\right|_{\delta p_c = \delta p_f^{(1)} = 0}. \tag{3}$$

It is the volume of fluid added to the matrix per unit bulk volume as the fractures are pressurized while maintaining constant external stress and constant pore fluid pressure in the matrix. The cross-storage term in the stress-based formulation is small because the total sample volume is free to expand (Fig. 1). Assuming $a_{23} \cong 0$ satisfactorily establishes the required sixth condition.

This result is in contrast to the Wilson and Aifantis assumption in the strain-based formulation that the cross-storage coefficient,

$$A_{23} = \left.\frac{\delta\zeta^{(1)}}{\delta p_f^{(2)}}\right|_{\delta\varepsilon = \delta p_f^{(1)} = 0}, \tag{4}$$

is negligible at constant volumetric strain (Fig. 2). Significant coupling occurs between the fracture and matrix for conditions of constant total strain. It will be shown in the discussion section that models assuming $A_{23} = 0$ produce unrealistic results.

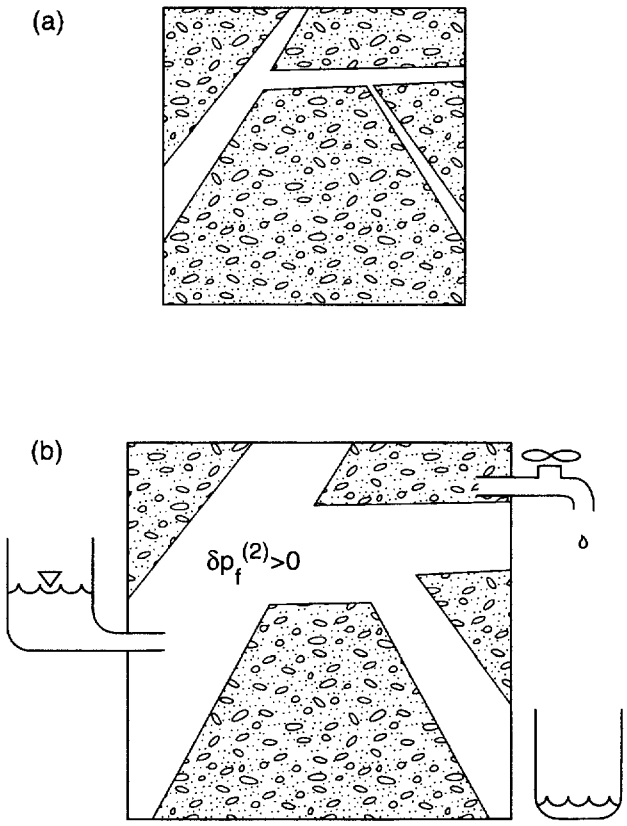

Fig. 1. Schematic figure representing an increase in fracture pressure of a double-porosity rock at constant external stress. (a) Reference state. (b) Increase in fracture pressure $\delta P_f^{(2)}$. Because the total volume is free to expand, the change in fluid mass is small, and hence, the cross-storage coefficient is small.

GOVERNING EQUATIONS FOR UNIAXIAL STRAIN

The one-dimensional column consolidation problem incorporates special conditions, which simplify the mathematics, and illustrates the significance of the cross-coupling storage coefficient. Van der Kamp and Gale (1983) showed that uniaxial strain conditions in a homogeneous single-porosity material reduce a coupled, inhomogeneous pressure diffusion equation to an uncoupled, homogeneous diffusion equation. Analogous simplifications are used in this derivation with the inclusion of additional terms to account for a double-porosity material.

The one-dimensional column is composed of double-porosity rocks of height, h (Fig. 3). Poroelastic boundary value problems require both a fluid boundary condition (pressure or flow) and a mechanical boundary condition (stress or displacement). For the column problem, there is a no flow boundary everywhere except the top. The fracture and matrix phases start with zero pore pressure. The top boundary is maintained at a constant pore pressure of zero in both the fracture and matrix. A constant stress (positive in extension) is applied to the top boundary. The bottom boundary has no vertical displacement while the sides have no horizontal displacement.

The poroelastic constitutive equation for strain written in terms of stress and pore fluid pressure for a double-porosity rock can be expressed as

$$\varepsilon_{ij} = \frac{1}{2G}\left(\sigma_{ij} - \frac{\nu}{1+\nu}\sigma_{kk}\delta_{ij}\right) - \frac{a_{12}}{3}p_f^{(1)}\delta_{ij} - \frac{a_{13}}{3}p_f^{(2)}\delta_{ij} \tag{5}$$

where σ_{kk} is the sum of the principal stresses and δ_{ij} is the Kronecker delta. Equation (5)

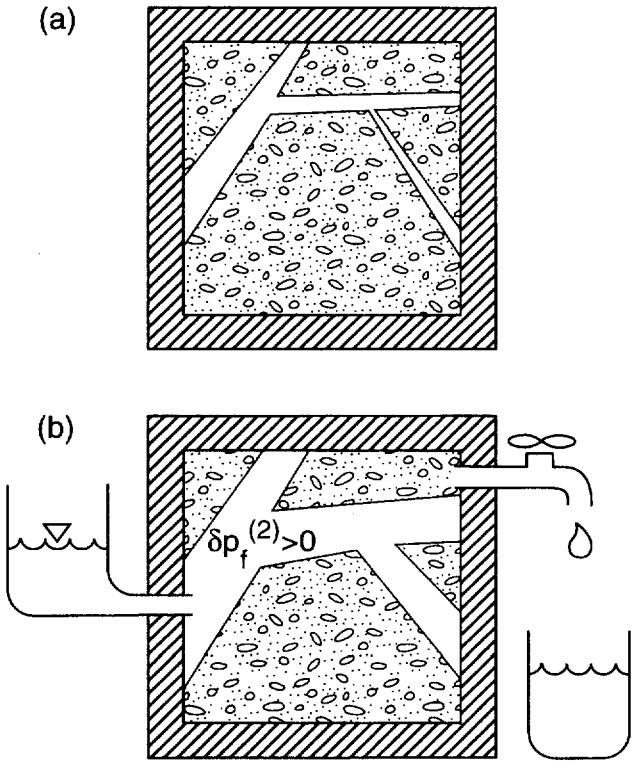

Fig. 2. Schematic figure representing an increase in fracture pressure of a double-porosity rock at constant volumetric strain. (a) Reference state. (b) Increase in fracture pressure $\delta P_f^{(2)}$. As the fracture volume expands, the matrix must contract and expel fluid. Hence, the cross-storage coefficient is significant.

generalizes eqn (2) to include shear strains and stresses. It is assumed that neither $p_f^{(1)}$ nor $p_f^{(2)}$ influence shear strain. The parameters G and ν are introduced as the shear modulus and Poisson's ratio of the combined fracture–matrix system. Stress, strain and fluid pressure are all taken to be changes relative to a reference state. The uniaxial strain boundary condition requires

$$\varepsilon_{22} = \varepsilon_{33} = 0. \tag{6}$$

The sum of the principal stresses can be written as a linear combination of the applied stress and the pore fluid pressure in the matrix and fracture when the conditions of eqn (6) are applied to eqn (5),

$$\sigma_{kk} = \left(\frac{1+\nu}{1-\nu}\right)\sigma_{11} + \eta a_{12} p_f^{(1)} + \eta a_{13} p_f^{(2)} \tag{7}$$

where

$$\eta = \frac{4G}{3}\left(\frac{1+\nu}{1-\nu}\right) = \frac{2(1-2\nu)}{a_{11}(1-\nu)}. \tag{8}$$

Constant stress

The condition of constant stress, $\sigma_{11} = 0$, applies at all times except at the instant of loading. For all times greater than $t = 0$, the mean stress can then be written as a linear function of the sum of the two fluid pressures

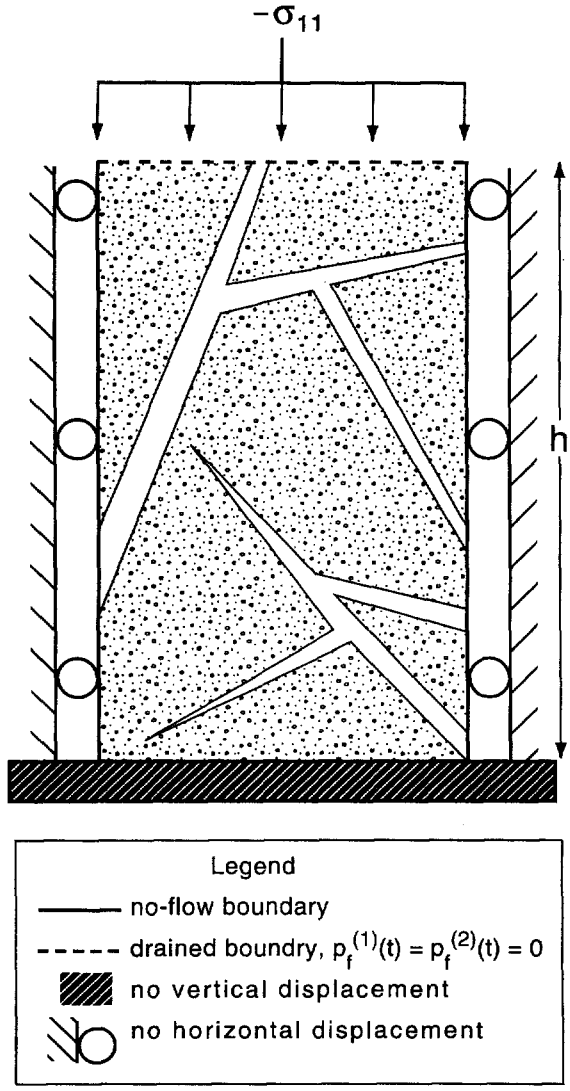

Fig. 3. Schematic representation of the column consolidation problem.

$$\frac{\sigma_{kk}}{3} = \frac{\eta}{3}(a_{12}p_f^{(1)} + a_{13}p_f^{(2)}). \tag{9}$$

Equation (9) is the double-porosity generalization of the single-porosity result given by Van der Kamp and Gale (1983) that mean stress is proportional to pore pressure. The consequence of applying the uniaxial strain and constant vertical stress conditions is that the pore pressure equations uncouple from the stress equations.

Substituting eqn (9) into (2) and defining the confining pressure as $p_c = -(\sigma_{kk}/3)$ yields

$$\zeta^{(1)} = \psi_{11}p_f^{(1)} + \psi_{12}p_f^{(2)} \tag{10}$$

and

$$\zeta^{(2)} = \psi_{21}p_f^{(1)} + \psi_{22}p_f^{(2)} \tag{11}$$

where

$$\psi_{11} = a_{22} - \frac{\eta}{3} a_{12}^2 \tag{12}$$

$$\psi_{12} = \psi_{21} = a_{23} - \frac{\eta}{3} a_{12} a_{13} \tag{13}$$

$$\psi_{22} = a_{33} - \frac{\eta}{3} a_{13}^2. \tag{14}$$

The increment of fluid content may also be expressed using continuity and Darcy's law as

$$\frac{\partial \zeta^{(1)}}{\partial t} = \frac{k_1}{\mu} \frac{\partial^2 p_f^{(1)}}{\partial x^2} + \kappa(p_f^{(2)} - p_f^{(1)}) \tag{15}$$

and

$$\frac{\partial \zeta^{(2)}}{\partial t} = \frac{k_2}{\mu} \frac{\partial^2 p_f^{(2)}}{\partial x^2} - \kappa(p_f^{(2)} - p_f^{(1)}) \tag{16}$$

where k_1 and k_2 are the permeabilities of the matrix and fracture, respectively, and μ is the fluid viscosity. The second term in eqns (15) and (16) is a cross-flow term proportional to the difference in pressure between the fracture and matrix, where κ is the constant of proportionality (Warren and Root, 1963). Fluid flow between the matrix and fracture is proportional to their pressure difference.

Two coupled diffusion equations are obtained by taking the time derivatives of eqns (10) and (11) and substituting them in eqns (15) and (16):

$$\frac{k_1}{\mu} \frac{\partial^2 p_f^{(1)}}{\partial x^2} + \kappa(p_f^{(2)} - p_f^{(1)}) = \psi_{11} \frac{\partial p_f^{(1)}}{\partial t} + \psi_{12} \frac{\partial p_f^{(2)}}{\partial t}, \tag{17}$$

$$\frac{k_2}{\mu} \frac{\partial^2 p_f^{(2)}}{\partial x^2} - \kappa(p_f^{(2)} - p_f^{(1)}) = \psi_{21} \frac{\partial p_f^{(1)}}{\partial t} + \psi_{22} \frac{\partial p_f^{(2)}}{\partial t}. \tag{18}$$

These equations have the same mathematical form as the strain-based eqns (3.6) of Wilson and Aifantis (1982) even though they neglected the cross-storage term A_{23}. Equations (17) and (18) generalize the result to include the cross-storage term. No assumption concerning the magnitude of the coupling between the matrix and fracture has been made in the derivation. The significance of the cross-storage term assumptions is evaluated in the discussion section.

ANALYTICAL SOLUTION

The solution to the consolidation problem consists of three parts: (1) the undrained response caused by the sudden application of the load; (2) the transient response due to fluid flow to the drain; and (3) the final drained response when there is no additional change in the column fluid pressure. The solution to each stage of consolidation behavior is given for the total displacement, and the pore pressure in the matrix and fractures, respectively. The solutions are presented for both the double-porosity and equivalent single-porosity medium to facilitate comparisons.

Undrained response—double-porosity

The undrained response occurs at loading when the increment of fluid content in both the matrix and fracture is zero. The pore fluid pressures and the axial strain can be solved by substituting eqn (7) into the constitutive eqns (6) and (5) and setting $\zeta^{(1)} = \zeta^{(2)} = 0$. Solutions for the undrained pore fluid pressures in the matrix, $p_u^{(1)}$, and fracture, $p_u^{(2)}$, are

$$p_u^{(1)} = \gamma^{(1)}\sigma_{11}, \tag{19}$$

$$p_u^{(2)} = \gamma^{(2)}\sigma_{11} \tag{20}$$

where

$$\gamma^{(1)} = \frac{3(1+\nu)a_{12}B^{(1)}}{[4G(1+\nu)a_{12}^2 - 9(1-\nu)a_{22}]B^{(1)} + [4G(1+\nu)a_{12}a_{13} - 9(1-\nu)a_{23}]B^{(2)}} \tag{21}$$

$$\gamma^{(2)} = \frac{3(1+\nu)a_{13}B^{(2)}}{[4G(1+\nu)a_{13}^2 - 9(1-\nu)a_{33}]B^{(2)} + [4G(1+\nu)a_{12}a_{13} - 9(1-\nu)a_{23}]B^{(1)}} \tag{22}$$

$$B^{(1)} = \frac{a_{13}a_{23} - a_{12}a_{33}}{a_{22}a_{33} - a_{23}^2} \simeq -\frac{a_{12}}{a_{22}} \tag{23}$$

$$B^{(2)} = \frac{a_{12}a_{23} - a_{13}a_{22}}{a_{22}a_{33} - a_{23}^2} \simeq -\frac{a_{13}}{a_{33}} \tag{24}$$

$B^{(1)}$ and $B^{(2)}$ are Skempton's coefficients for the matrix and fracture, respectively. The coefficients $\gamma^{(1)}$ and $\gamma^{(2)}$ are loading efficiencies for the matrix and the fracture, respectively, when the bulk material is in a state of uniaxial strain. They are the ratio of the undrained response of pore pressure to axial loading with negligible horizontal displacements. Each loading efficiency term reduces to the single-porosity loading efficiency parameter defined by Van der Kamp and Gale (1983) as one of the porosities goes to zero.

The undrained axial strain is

$$\varepsilon_{11}^{(u)} = \varepsilon_{kk}^{(u)} = \frac{(1+\nu)}{3(1-\nu)}[a_{11}\sigma_{11} - a_{12}p_u^{(1)} - a_{13}p_u^{(2)}]. \tag{25}$$

Taking the ratio $\varepsilon_{11}^{(u)}/\sigma_{11}$ defines the undrained uniaxial compressibility,

$$\frac{1}{K_v^{(u)}} = \frac{(1+\nu)}{3(1-\nu)}[a_{11} - a_{12}\gamma^{(1)} - a_{13}\gamma^{(2)}]. \tag{26}$$

The initial displacement at the top of the column due to the instantaneous loading under undrained conditions is

$$U^{(u)} = U_T(0,0) = -\frac{\sigma_{11}h}{K_v^{(u)}}. \tag{27}$$

Undrained response—long time

The behavior of a double-porosity system can be analyzed by assuming the material can be considered homogeneous at some appropriate larger time scale. A long-duration undrained test of a double-porosity rock produces the same physical results as an equivalent single-porosity rock. The coefficients of the equivalent material are defined as

$$a_{11}^* = a_{11} \tag{28}$$

$$a_{12}^* = a_{12} + a_{13} \tag{29}$$

$$a_{22}^* = a_{22} + 2a_{23} + a_{33} \tag{30}$$

where the asterisk represents parameters for the equivalent homogeneous material. The undrained uniaxial pore pressure, p_u^*, is

$$p_u^* = \gamma^* \sigma_{11} \tag{31}$$

where the loading efficiency for the state of uniaxial strain is

$$\gamma^* = \frac{3(1+\nu)a_{12}^*}{9(1-\nu)a_{22}^* - 4G(1+\nu)a_{12}^* a_{12}^*}. \tag{32}$$

The undrained axial strain for the equivalent material is

$$\varepsilon_{11}^{(u)*} = \frac{(1+\nu)}{3(1-\nu)}[a_{11}^* \sigma_{11} - a_{12}^* p_u^*]. \tag{33}$$

Taking the ratio of $\varepsilon_{11}^{(u)*}/\sigma_{11}$ defines the equivalent undrained uniaxial compressibility

$$\frac{1}{K_v^{(u)*}} = \frac{(1+\nu)}{3(1-\nu)}[a_{11}^* - a_{12}^* \gamma^*]. \tag{34}$$

The initial displacement at the top of the column due to the instantaneous loading under undrained conditions is

$$U^{(u)*} = -\frac{\sigma_{11} h}{K_v^{(u)*}}. \tag{35}$$

Transient solution—double-porosity

Wilson and Aifantis (1982) derived analytical solutions for the pore fluid pressure in the matrix and fracture, and the vertical displacement due to column consolidation using a strain-based formulation. Analytical solutions are derived for the stress-based formulation using analogous methods.

The coupled eqns (17) and (18) can be solved using the finite Fourier transform pair

$$\bar{p}(n, t) = \int_0^h p(x, t) \sin\frac{(2n+1)\pi x}{2h} \mathrm{d}x \tag{36}$$

$$p(x, t) = \frac{2}{h} \sum_{n=0}^{\infty} \bar{p}(n, t) \sin\frac{(2n+1)\pi x}{2h}. \tag{37}$$

Application of the forward transform results in two coupled first order differential equations which can be solved by ordinary techniques (Wilson and Aifantis, 1982). The pore fluid pressure solutions are

$$p_f^{(1)} = \frac{2}{h} \sum_{n=0}^{\infty} [\omega_1 e^{z_1 t} - \omega_2 e^{z_2 t}] \sin\frac{(2n+1)\pi x}{2h}, \tag{38}$$

and

$$p_f^{(2)} = \frac{2}{h}\sum_{n=0}^{\infty}\left[\omega_1\left(\frac{-D_{21}}{D_{22}-Z_1}\right)e^{Z_1 t}-\omega_2\left(\frac{-D_{21}}{D_{22}-Z_2}\right)e^{Z_2 t}\right]\sin\frac{(2n+1)\pi x}{2h} \tag{39}$$

where

$$\omega_1 = \frac{p_u^{(1)}}{m(Z_1-Z_2)}\left(-D_{22}+Z_1+\frac{p_u^{(2)}}{p_u^{(1)}}D_{12}\right) \tag{40}$$

$$\omega_2 = -\frac{p_u^{(2)}}{m(Z_1-Z_2)}\left(D_{12}+\frac{p_u^{(1)}}{p_u^{(2)}}(D_{11}-Z_1)\right) \tag{41}$$

$$Z_1 = (D_{11}+D_{22})+[(-D_{11}-D_{22})^2-4(D_{11}D_{22}-D_{12}D_{21})]^{1/2} \tag{42}$$

$$Z_2 = (D_{11}+D_{22})-[(-D_{11}-D_{22})^2-4(D_{11}D_{22}-D_{12}D_{21})]^{1/2} \tag{43}$$

$$D_{11} = \frac{-m^2\left(\frac{k_1}{\mu}\right)\psi_{22}-\kappa(\psi_{22}-\psi_{12})}{\psi_{11}\psi_{22}-\psi_{12}^2} \tag{44}$$

$$D_{12} = \frac{m^2\left(\frac{k_2}{\mu}\right)\psi_{12}+\kappa(\psi_{22}+\psi_{12})}{\psi_{11}\psi_{22}-\psi_{12}^2} \tag{45}$$

$$D_{21} = \frac{m^2\left(\frac{k_1}{\mu}\right)\psi_{12}+\kappa(\psi_{12}+\psi_{11})}{\psi_{11}\psi_{22}-\psi_{12}^2} \tag{46}$$

$$D_{22} = \frac{-m^2\left(\frac{k_2}{\mu}\right)\psi_{11}-\kappa(\psi_{12}-\psi_{11})}{\psi_{11}\psi_{22}-\psi_{12}^2} \tag{47}$$

$$m = \frac{(2n+1)\pi}{2h}. \tag{48}$$

The total displacement field is calculated by integrating the vertical strain equation over the column length, applying the boundary conditions and substituting the pore fluid pressure solutions. The result is

$$U_T(0,t) = -\frac{a_{11}(1+\nu)\sigma_{11}h}{3(1-\nu)}+\frac{4(1+\nu)}{3\pi(1-\nu)}\sum_{n=0}^{\infty}\frac{1}{(2n+1)} \tag{49}$$

$$\times\left[\omega_1\left(a_{12}+\left(\frac{-D_{12}}{D_{22}-Z_1}\right)a_{13}\right)e^{Z_1 t}-\omega_2\left(a_{12}+\left(\frac{-D_{12}}{D_{22}-Z_2}\right)a_{13}\right)e^{Z_2 t}\right]. \tag{50}$$

The settlement due to consolidation is $U_c = U_T - U^{(u)}$.

Transient solution—single-porosity

The double-porosity formulas reduce to known single-porosity equations for an equivalent medium when the matrix–fracture interplay is steady state (Detournay and Cheng, 1993).

$$p_f^* = \frac{2p_u^*}{h}\sum_{n=0}^{\infty}\frac{1}{m}e^{\frac{-m^2k_{\uparrow}^*t}{\mu\psi_{\uparrow 1}^*}}\sin\frac{(2n+1)\pi x}{2h} \tag{51}$$

$$U_T^*(0,t) = -\frac{a_{11}\sigma_{11}h}{3}\left(\frac{1+\nu}{1-\nu}\right)+\frac{8a_{\uparrow 2}^*hp_u^*}{3\pi^2}\left(\frac{1+\nu}{1-\nu}\right)\sum_{n=0}^{\infty}\frac{1}{(2n+1)^2}e^{\frac{-m^2k_{\uparrow}^*t}{\mu\psi_{\uparrow 1}^*}}. \tag{52}$$

Drained response

The drained response occurs when there is no pore fluid pressure change, i.e., $p_f^{(1)} = p_f^{(2)} = 0$. The solutions for a double-porosity material are equivalent to single-porosity rocks at drained conditions. The axial strain is

$$\varepsilon_{11} = \frac{(1+\nu)}{3(1-\nu)}a_{11}\sigma_{11}. \tag{53}$$

The drained uniaxial compressibility is

$$\frac{1}{K_v^{(d)}} = \frac{a_{11}}{3}\left(\frac{1+\nu}{1-\nu}\right). \tag{54}$$

The total displacement for drained conditions is

$$U^{(d)} = -\frac{\sigma_{11}h}{K_v^{(d)}}. \tag{55}$$

RESULTS

Numerical results are calculated using two separate methods to check for numerical accuracy and consistency. One method is to evaluate directly the analytical solutions derived in the previous section. The accuracy of the analytical results depends on the number of terms in the infinite sum. A large number of terms is required at short times, but the solution is more robust as time increases. A second method is to solve eqns (17) and (18) using a Crank–Nicolson finite difference approximation. A bitridiagonal matrix routine is used to handle the coupled nature of the equations. The solution is accurate in the order of the square of the time and spatial sampling internal ($O(\Delta t^2, \Delta x^2)$).

Table 1 shows rock properties for Berea sandstone. These values and fracture properties are used in calculating the double-porosity model parameters shown in Table 2. The

Table 1. Berea sandstone properties

Parameter	Value
$K^{(1)}$, GPa	8.0[a]
K_f, GPa	3.3[a]
K_s, GPa	36.0[a]
$\nu^{(1)}$	0.2[a]
$\phi^{(1)}$	0.064[b]
$\alpha^{(1)}$	0.78[c]
$B^{(1)}$	0.847[c]

[a] From Rice and Cleary, 1976.
[b] From Touloukian *et al.*, 1989.
[c] From Berryman and Wang, 1995.

Table 2. Double-porosity model parameters calculated using Berea sandstone properties and estimated fracture properties (Berryman and Wang, 1995)

Parameter	Formula	Value
L, m		0.1
s_n, GPa/m		12.1
s_s, GPa/m		10.0
G, GPa		0.857
ν		0.18
$v^{(1)}$	$1-v^{(2)}$	0.9936
$v^{(2)}$	$0.1\phi^{(1)}$	0.0064
$K^{(2)}$, GPa	$s_n L v^{(2)}$	0.00774
a_{11}, 1/GPa	$1/K$	0.951
a_{12}, 1/GPa	$-v^{(1)}\alpha^{(1)}/K^{(1)}$	−0.0969
a_{13}, 1/GPa	$-v^{(2)}/K^{(2)}$	−0.826
a_{22}, 1/GPa	$v^{(1)}\alpha^{(1)}/B^{(1)}K^{(1)}$	0.1144
a_{23}, 1/GPa		0.0
a_{33}, 1/GPa	$v^{(2)}(1/K_f+1/K^{(2)})$	0.828
k_1/μ, m²/GPa s		0.0001
k_2/μ, m²/GPa s		1.0
κ, 1/GPa s		0.06

constant stress cross-storage coefficient a_{23} is assumed to be zero (Berryman and Wang, 1995). Values of the shear modulus and Poisson's ratio of the combined matrix–fracture system are determined using the bulk modulus and Poisson's ratio of the matrix and assumed shear stiffness,

$$G = \frac{G^{(1)} s_s L}{(G^{(1)} + s_s L)} \tag{56}$$

(Goodman, 1980) and

$$\nu = \frac{3K - 2G}{2(3K+G)}, \tag{57}$$

where

$$G^{(1)} = \frac{3K^{(1)}(1-2\nu^{(1)})}{2(1+\nu^{(1)})}. \tag{58}$$

The cross-flow parameter, κ, is defined by the relation

$$\kappa = \frac{\vartheta k_1}{L^2 \mu} \tag{59}$$

where ϑ is a parameter which reflects the geometry of the matrix block. Output from the modeled parameters is examined followed by parameter sensitivity results. Normalized and dimensionless plots are used to generalize the results. Fluid pressures are normalized to the magnitude of the applied stress. Displacements are normalized to the total surface displacement at drained conditions. Depths are normalized to the maximum column height. Dimensionless time is defined by the formula

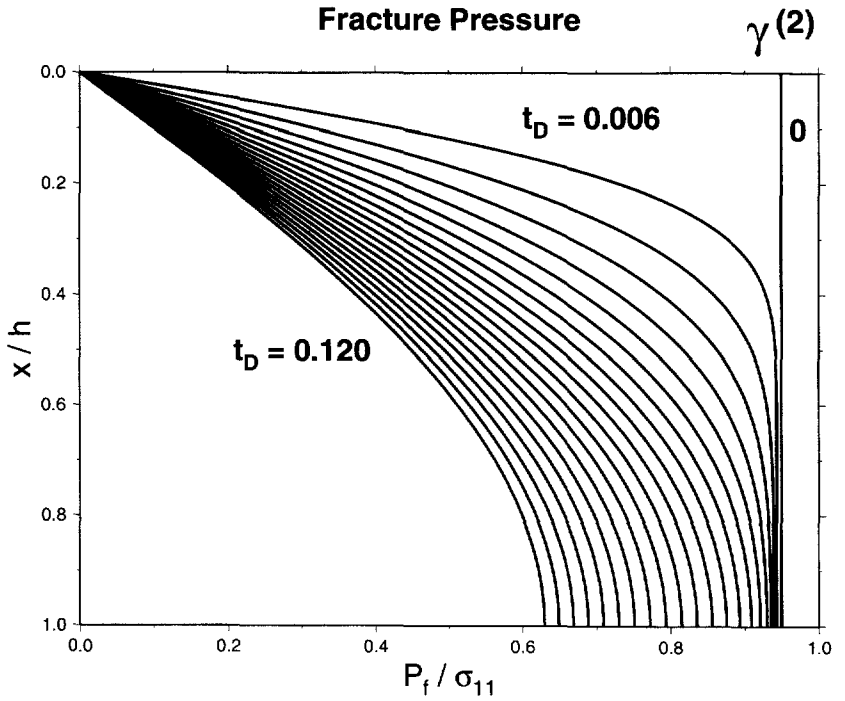

Fig. 4. Fluid pressure response in the fracture phase at twenty-one different times. The dimensionless time increment is $t_D = 0.006$.

$$t_D = \frac{k}{\mu S h^2} t \tag{60}$$

where S is the total storage coefficient, $S = S_1 + S_2 = a_{22} + a_{33}$, and k is the total permeability, $k = k_1 + k_2$.

Figure 4 is a plot of the fluid pressure distribution with depth in the fracture phase at twenty-one different times. The undrained fluid pressure response is 95% of the applied vertical load and is constant throughout the column. The twenty remaining curves show the fracture pressure distribution at evenly spaced dimensionless time increments of $t_D = 0.006$. Fracture fluid pressure at every depth decreases with increasing time. The fractures have a high conductivity and the fluid pressure distribution changes rapidly. The bottom of the column responds more slowly than the upper section due to the increased distance to the fluid outlet at the top of the column.

Figure 5 is the corresponding plot for the matrix pore fluid pressure distribution with depth. The instantaneous undrained response in the matrix at the time the load is suddenly applied is a constant throughout the column. The pressure is 81% of the applied load or 14% lower than the undrained fracture fluid pressure response. A positive pressure gradient exists between the fracture and matrix material resulting in flow out of the fracture and into the matrix at all depths initially. The high conductivity of the fracture causes fluid to exit the system quickly at the shallow depths reducing and changing the sign of the pressure differential between the fracture and matrix, which inhibits significant build up of matrix pressure. At depths farther from the fluid drain, however, cross-flow occurs for long times resulting in measurable matrix pressure buildup. Pressure in the fracture decreases more rapidly than the pressure in the matrix due to the fracture's higher permeability. Eventually, the fluid pressure in the fracture is less than the fluid pressure in the matrix throughout the column. Matrix pressures slowly decay by matrix flow toward the top and cross-flow into the fractures.

The relationships between the fracture and matrix pressures are clearly seen in Fig. 6 for depths of 0.4 h and 0.9 h below the top of the column. For each depth, the fracture

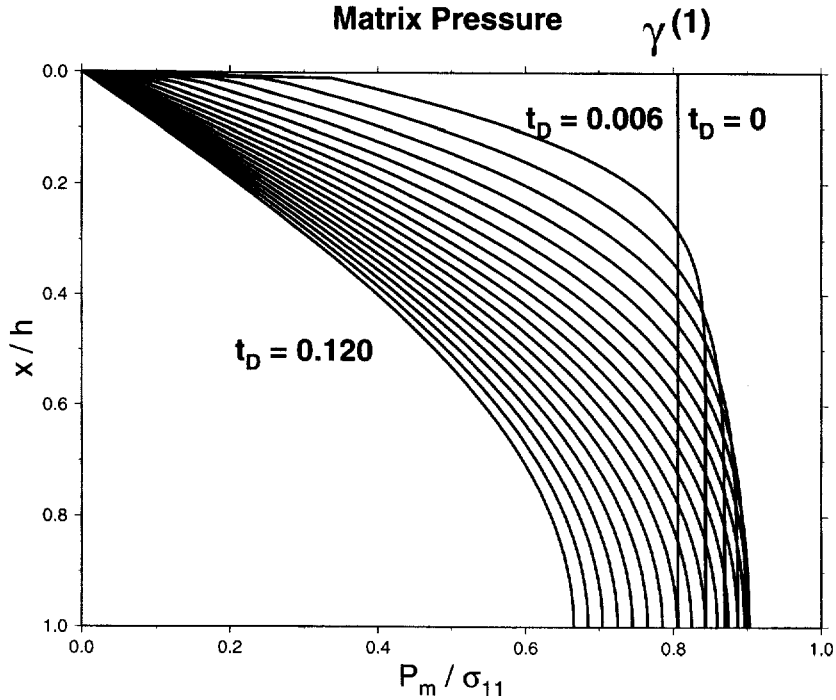

Fig. 5. Pore fluid pressure response in the matrix phase at twenty-one different times. The constant dimensionless time increment is 0.006.

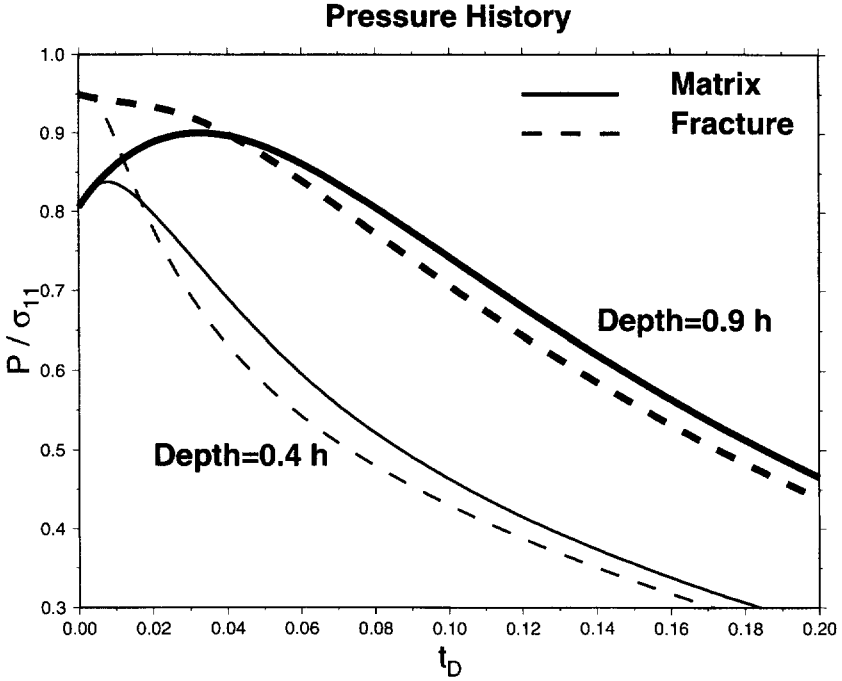

Fig. 6. Pore fluid pressure histories at two separate depths below the surface, 0.4 h (thin line) and 0.9 h (thick line). Solid lines show matrix pore fluid pressure whereas dashed lines represent the fracture fluid pressure.

pressure is initially greater than that of the matrix. This pressure gradient induces flow from the fractures into the matrix until the two curves cross. The rapid crossover in the pressure differential between the fracture and the matrix at shallow depths causes nominal pressure

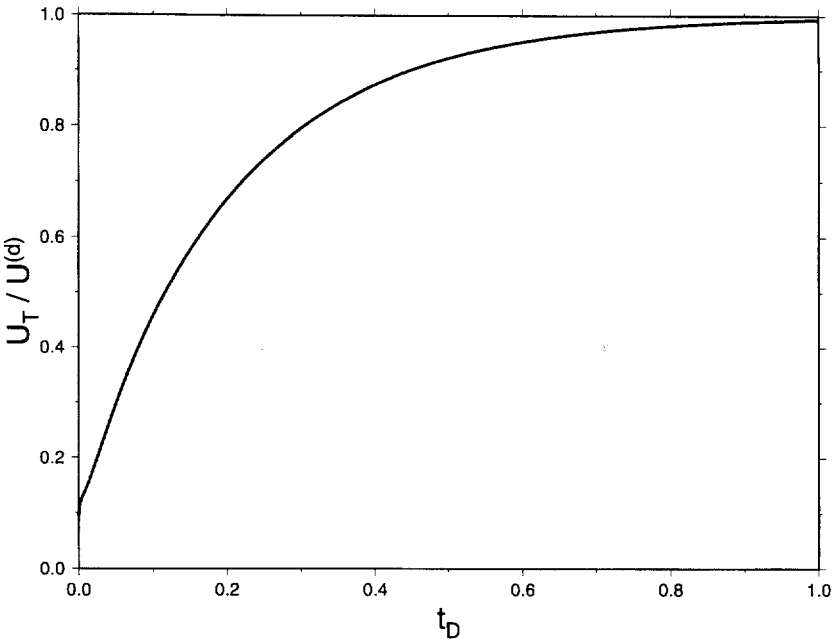

Fig. 7. Total surface displacement for a column composed of a double-porosity material when a constant vertical load is applied with negligible horizontal displacement. The discontinuity at zero time is the undrained response.

increases in the matrix. The maximum matrix pore fluid pressure occurs early in time. The fluid pressure crossover time at 0.9 h is delayed compared to 0.4 h because the fracture flow path to the fluid drain is longer. This long duration pressure gradient causes a 10% increase in the matrix fluid pressure. A column model without the fluid drain has a normalized equilibrium pressure of 0.93. The high conductivity of the fracture causes rapid changes in pressure within the fracture relative to the lower permeability matrix blocks. The pressure gradient reverses sign at all times greater than the instant of crossover inducing fluid flow out of storage in the matrix and into the fractures.

Figure 7 shows the normalized total surface displacement as a function of dimensionless time. The instantaneous displacement that occurs at the instant of loading is 9% of the maximum total surface displacement at drained conditions. The greatest rate of consolidation occurs during early time. The drained displacement is approximated by the asymptotic curve during late time.

Model parameter sensitivity

The effects of varying fracture spacing, contrast in permeability between the fracture and matrix, magnitude of cross-flow, and matrix porosity are investigated. A pressure history at 0.5 h and a displacement history are plotted for each case.

Fracture spacings of 0.01 and 1.00 m are compared to the original spacing of 0.1 m (Figs 8 and 9). An increase in the distance between the fractures decreases the total compressibility and total permeability of the combined matrix–fracture system. Longer fracture spacing also reduces the instantaneous buildup of fluid pressure in both the matrix and fracture, reduces the initial pressure gradient between matrix and fracture, and decreases the cross-flow term. Matrix pressure decreases slowly due to the reduced surface area of cross-flow and the increased flow distance to a fracture. Closely spaced fractures increase the fractured rock compressibility, the undrained fluid pressures, the initial gradient between the matrix and fracture, and the cross-flow between the two phases. The matrix phase equilibrates with the fracture phase quickly. Pressure equilibration is maintained because of the large surface area for cross-flow and the short flow distance to fractures.

Permeability variations are examined by holding the matrix permeability constant and decreasing the intrinsic permeability of a single fracture by one and two orders of magnitude.

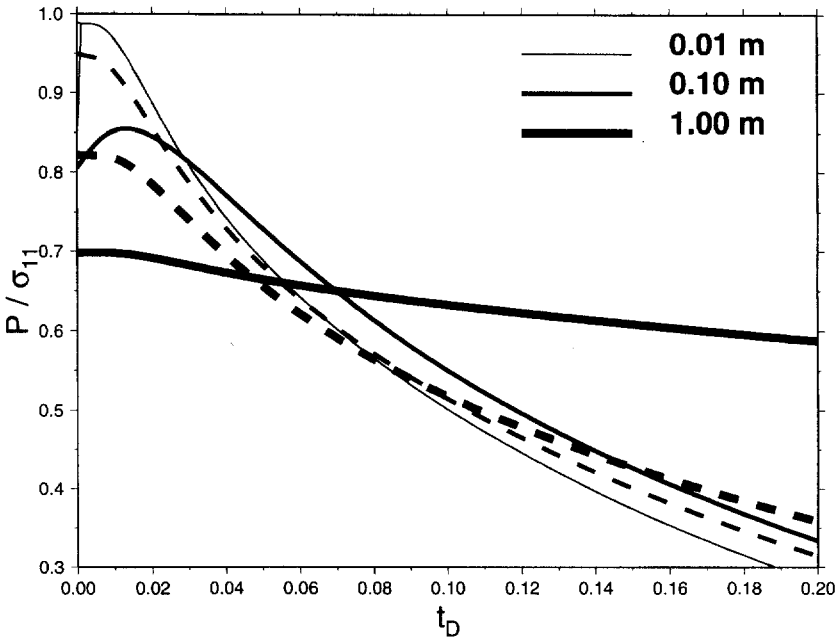

Fig. 8. Pressure histories at a depth of 0.5 h for three different fracture spacings. Solid lines are for the matrix phase and the dashed lines are for the fracture phase. The matrix and fracture phase pressures equilibrate rapidly for closely spaced fractures (0.01 m).

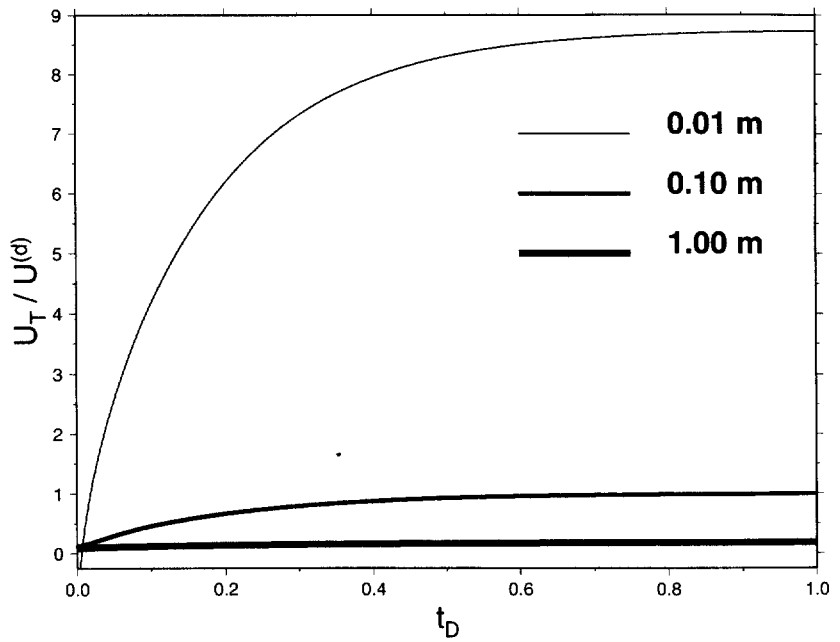

Fig. 9. Total surface displacement variations caused by fracture spacing changes. $U^{(d)}$ is the total surface displacement for drained conditions using a fracture spacing of 0.10 m.

The magnitude of the cross-flow parameter in unaffected by fracture permeability perturbations because κ is a function of matrix permeability, fluid viscosity, fracture spacing, and the surface area flow geometry [eqn (59)]. Decreasing the fracture to matrix permeability ratio reduces the fracture's ability to preferentially drain relative to the matrix. Fluid moves less rapidly through the fractures to the drain at the top of the column (Fig.

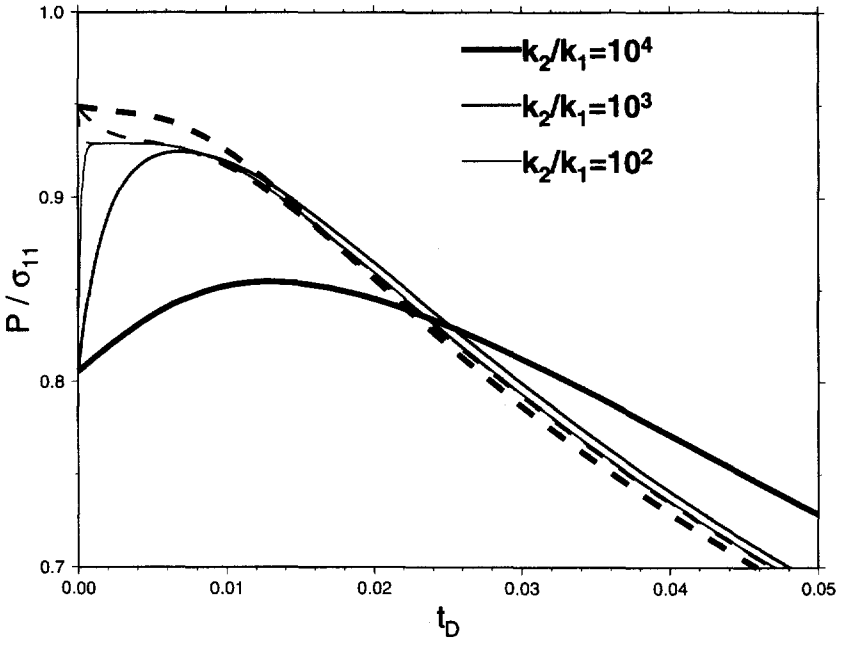

Fig. 10. Pressure histories at a depth of 0.5 h for three different fracture-to-matrix permeability ratios. Solid lines are for the matrix phase and dashed lines are for the fracture phase.

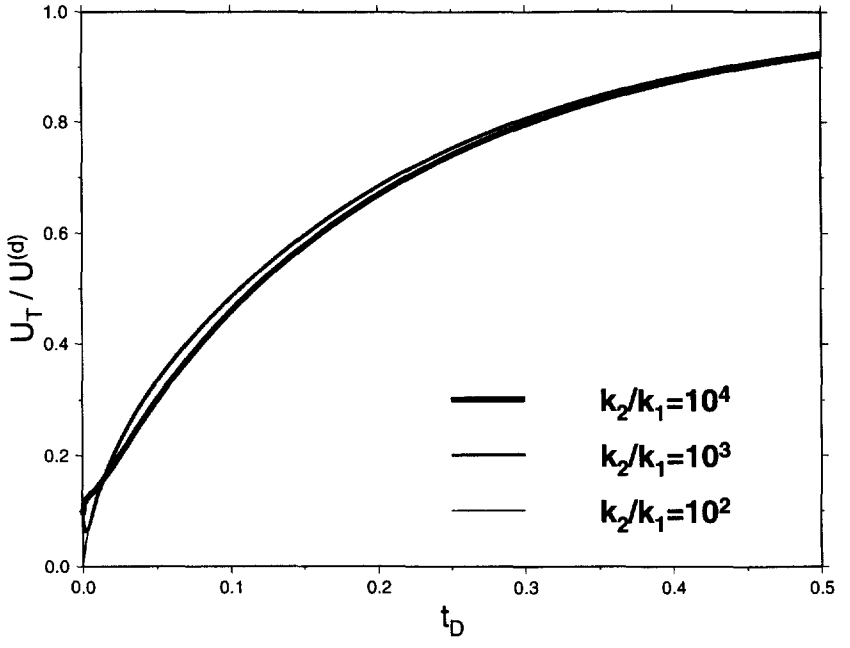

Fig. 11. Total surface displacement variations due to fracture-to-matrix permeability ratio changes.

10). More fluid flows out of the fractures and into the matrix which forces the matrix pore fluid pressure to rise. Pressure gradients and, hence, cross-flow is reduced once the matrix pressure approaches the fracture pressure. The volumetric expansion observed for low permeability contrasts is caused by the increase in matrix phase pressure (Fig. 11).

The cross-flow parameter, κ, is assumed to be a function of the matrix permeability, fluid viscosity, fracture spacing, and surface area flow geometry. A skin factor at the matrix–fracture interface may reduce the rate of cross-flow. Manifestations of cross-flow

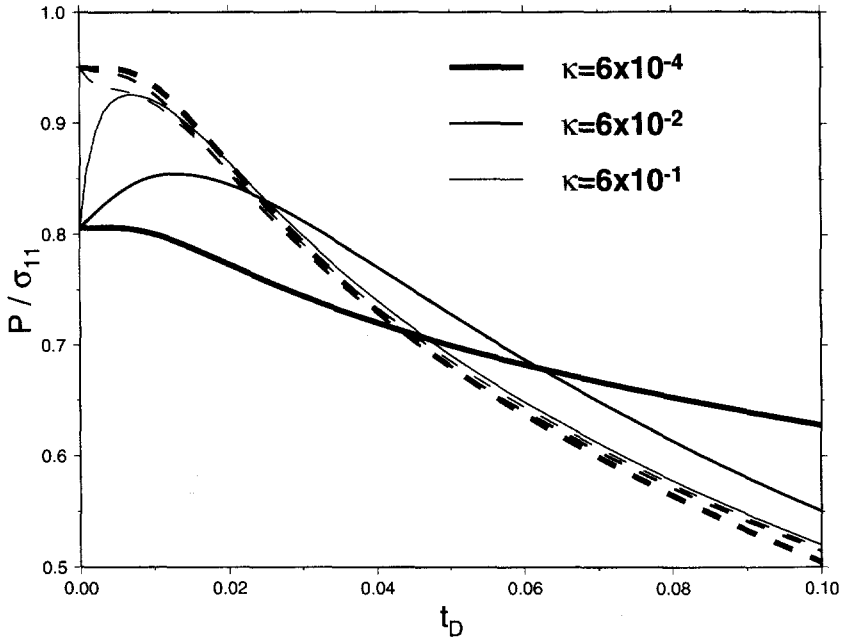

Fig. 12. Pressure histories at a depth of 0.5 h for three different cross-flow terms. Solid lines are for the matrix phase and dashed lines are for the fracture phase.

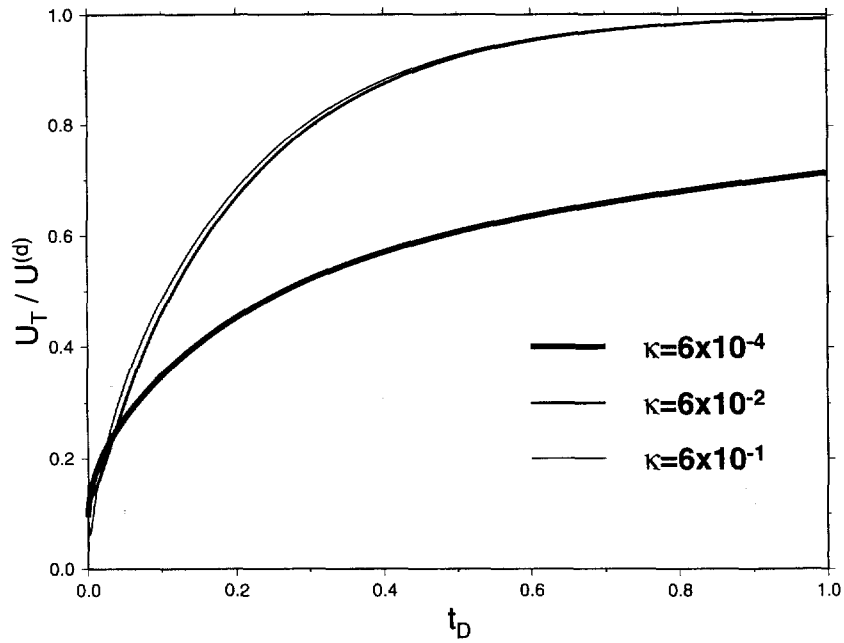

Fig. 13. Total surface displacement variations caused by cross-flow changes.

perturbations are seen in Figs 12 and 13. High κ values represent high rates of cross-flow, which increases the matrix pore fluid pressure to increase until it crosses over the fracture fluid pressure. Low pressure gradients are maintained after the initial crossover. Although the large buildup of matrix pressure causes slight volume expansion, rapid cross-flow utilizes the fracture's high permeability resulting in rapid total pressure reduction and fast column consolidation. Low κ values reduce cross-flow. Fracture pressures drop rapidly, but matrix fluid pressures change slowly, which decreases the rate of column consolidation.

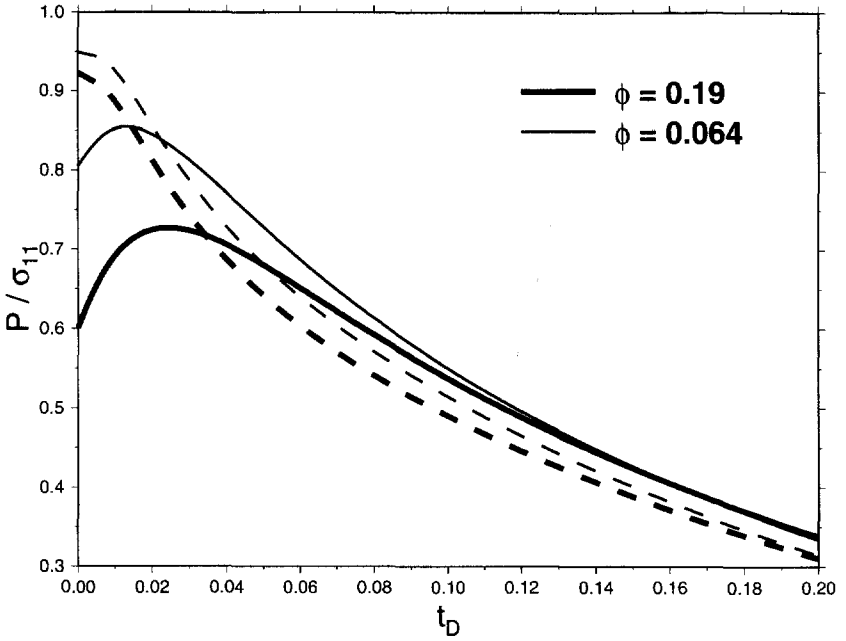

Fig. 14. Pressure histories at a depth of 0.5 h for $\phi^{(1)} = 0.064$ and $\phi^{(1)} = 0.19$. Solid lines are for the matrix phase and dashed lines are for the fracture phase.

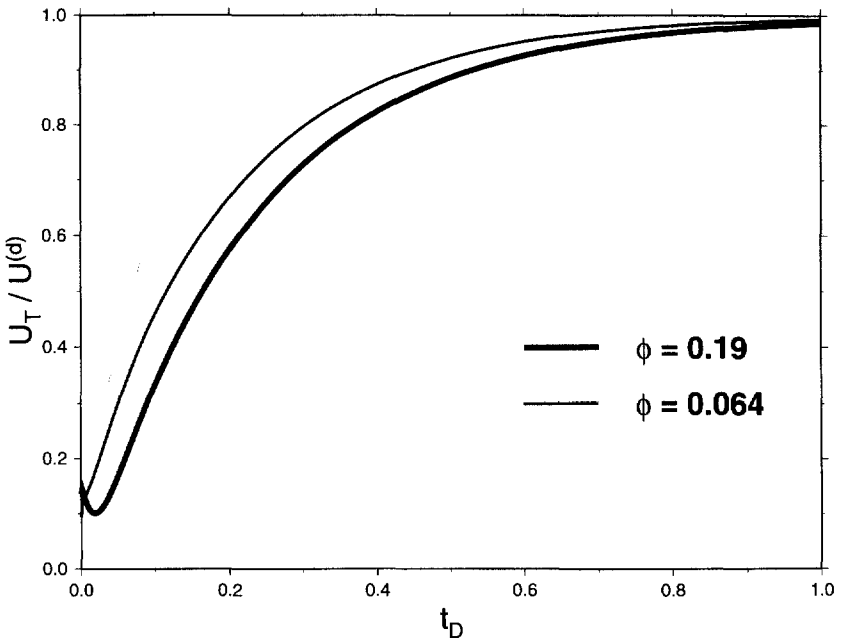

Fig. 15. Total surface displacement variations for $\phi^{(1)} = 0.064$ and $\phi^{(1)} = 0.19$. $U^{(d)}$ is the total surface displacement for drained conditions using the assumption of $a_{23} = 0$.

Figures 14 and 15 are the pressure and displacement histories for an increase in matrix porosity assuming no other parametric changes. The parameters used in the model are consistent with $\phi^{(1)} = 0.064$ as given by Berryman and Wang (1995) and Elsworth and Bai (1992). The poroelastic properties of Berea sandstone have been measured recently by Hart and Wang (1995) with the matrix porosity equal to 19% ($\phi^{(1)} = 0.19$). Increasing matrix porosity causes a small decrease in the matrix poroelastic expansion coefficient, a_{12} and a large increase in the matrix storage coefficient, a_{22}. Consequently, the matrix Skempton's

coefficient, $B^{(1)}$, is decreased. The instantaneous buildup of fluid pressure in the matrix is decreased. The initial pressure gradient between the matrix and fracture is higher which increases the cross-flow of fluid out of the fracture and into the matrix. The large pressure buildup in the matrix forces the column to expand. Consolidation is delayed relative to the low porosity case, but the rate of change in the displacement is similar once the matrix and fracture fluid pressures cross over and the pressure gradient reverses sign.

DISCUSSION

The constant stress and constant strain formulations are equivalent as long as no assumptions are made about the values of the material coefficients. Differences in the formulations exist only in the choice of whether strain or stress is the independent variable. The different formulations lead to different boundary conditions on the representative elementary volume for the storage coefficient tensor.

Several authors (Wilson and Aifantis, 1982; Khaled *et al.*, 1984; Beskos and Aifantis, 1986; Elsworth and Bai, 1990, 1992; Bai *et al.*, 1993) assume the constant strain cross-storage coefficient is negligible ($A_{23} = 0$). This assumption produces a small underestimation in the fracture pressure and a significant underestimation of the matrix pressure at short times (Fig. 16). The underestimation establishes an exaggerated pressure gradient between the matrix and fracture causing significant cross-flow of fluid out of the fracture and into the matrix. Matrix pressure increases by a factor of five. The extreme buildup in the matrix

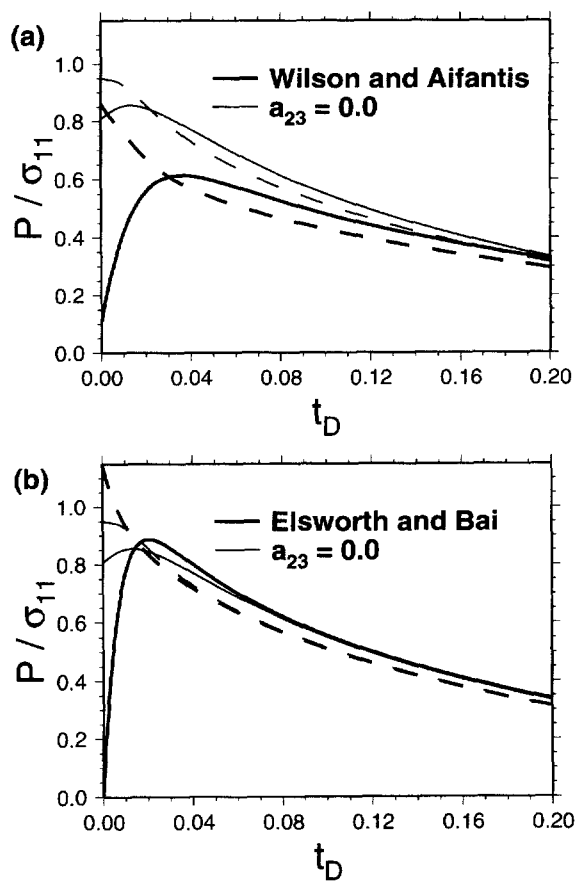

Fig. 16. A comparison of the fluid pressure histories for different storage coefficient assumptions. Solid lines are for the matrix phase and the dashed lines are for the fracture phase. The constant stress cross-storage coefficient a_{23} is assumed to be zero in the stress-based constitutive theory (thin lines). Alternative storage coefficient assumptions are made by other models (heavy lines) with (a) $A_{23} = 0$ ($a_{23} \neq 0$), and (b) $A_{23} = 0$ plus rigid fracture and rigid matrix volume.

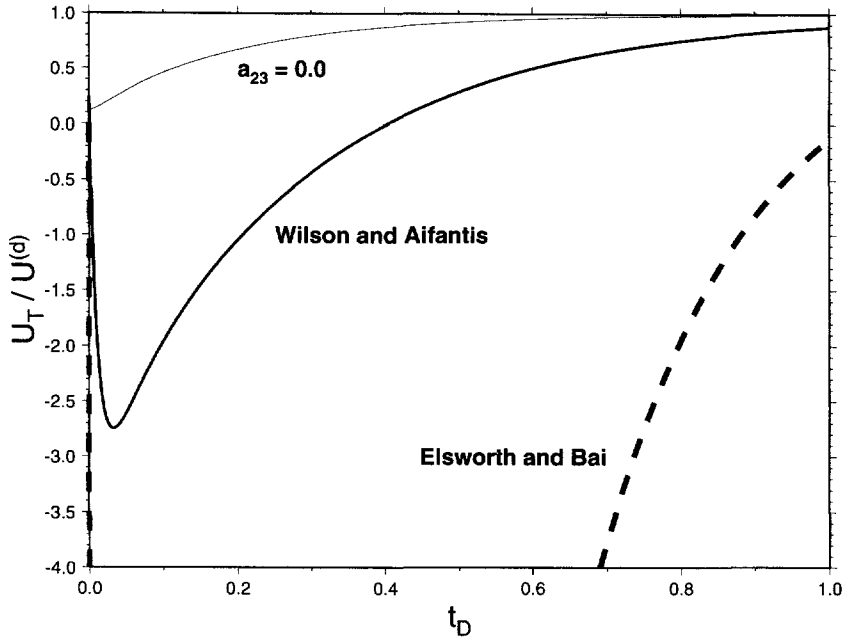

Fig. 17. A comparison of the total displacement histories for different storage coefficient assumptions. The constant stress cross-storage coefficient a_{23} is assumed to be zero in the stress-based constitutive theory (thin line). Alternative storage coefficient assumptions are made by other models $A_{23} = 0$ (heavy solid line) and $A_{23} = 0$ plus rigid fracture and rigid matrix volume (heavy dashed line).

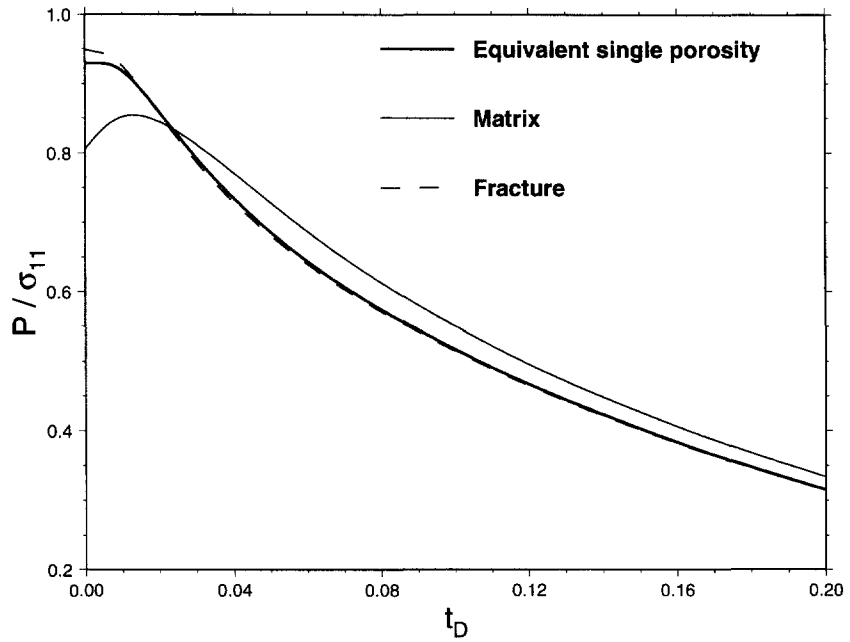

Fig. 18. A pressure history comparison between the double-porosity model and the equivalent single-porosity model. The pressure in the equivalent single-porosity model approximates the fracture pressure profile in the double-porosity model.

pressure causes the column to expand about three times the maximum consolidation (Fig. 17).

In addition to assuming that the constant strain cross-storage coefficient is negligible, Elsworth and Bai (1990, 1992) further assumed the constant strain fracture storage

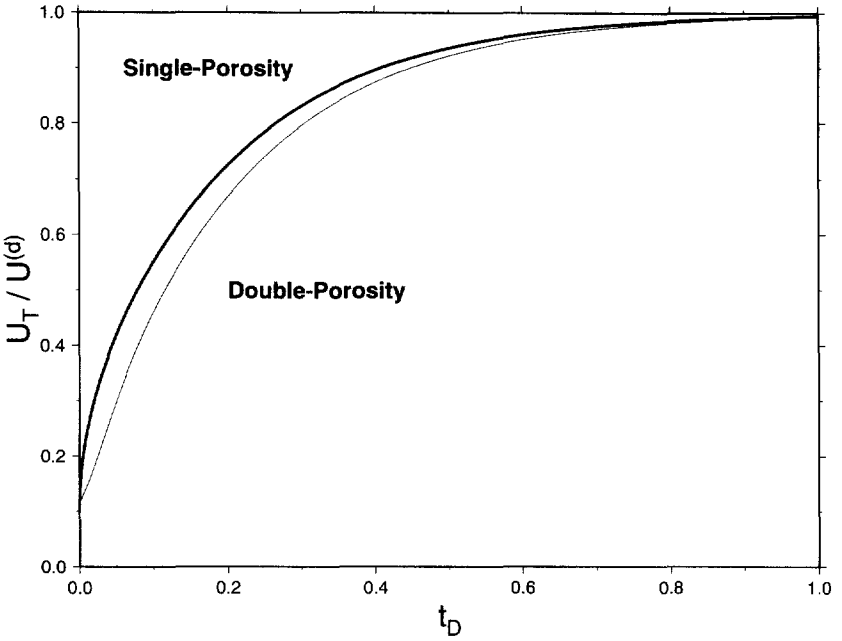

Fig. 19. A total surface displacement history comparison between the double-porosity model and the equivalent single-porosity model.

coefficient depends only on the fluid compressibility, $A_{33} = v^{(2)}/K_f$ (rigid fracture), when in fact the fractures can expand due to matrix contraction within the constraint of constant total strain. Additionally, they assumed that the constant strain matrix storage coefficient is a function of the compressibilities of the fluid and solid grains, $A_{22} = \phi^{(1)}/K_f + (1-\phi^{(1)})/K_s$ (rigid matrix volume). The early time pressure histories suggest negligible pressure buildup in the matrix and pressures in excess of the applied stress in the fracture (Fig. 16). The extreme gradient produces massive cross-flow, enormous matrix pressure buildup, and unreasonably large volumetric expansion (Fig. 17).

Equivalent single-porosity case

The equivalent single-porosity case is best used to show the long term, steady-state limit of a double-porosity model. The equivalent single-porosity rock has the total storage and permeability of the combined fracture–matrix system, but ignores the interaction between the fracture and matrix. Analysis of the equivalent single-porosity rock, therefore, highlights the significance of this interaction.

Except for the slightly lower initial values, the equivalent single-porosity pressure history mimics the fracture phase pressure curve of the double-porosity rock (Fig. 18). It should be remembered, however, that the volume fraction of the rock mass which is fractured is small compared to the total volume. Subsurface pressure measurements would, most likely, record values closer in magnitude to the matrix phase.

Furthermore, the rate of displacement for the double-porosity model is smaller than the equivalent single-porosity case (Fig. 19). Cross-flow in the double-porosity rock increases matrix fluid pressure causing a slight volumetric expansion. Consolidation of the double-porosity column remains positive, but reduced compared to the equivalent single-porosity model.

Equivalent single-porosity models are often used to approximate complex double-porosity rocks. Differences between the single-porosity and double-porosity models exist in the fluid pressure and displacement histories at early times before steady state cross-flow. Subsurface pressure measurements recorded in a truly double-porosity rock, but used for predictive modeling in an equivalent single-porosity model would produce unreliable displacement and pressure predictions. The magnitude of these differences is dependent on the volume and rate of fluid interaction between the matrix and fracture.

CONCLUSIONS

(1) Uniaxial strain and constant vertical stress conditions in the column consolidation problem imply that the mean stress is a linear combination of the two fluid pressures. This result is analogous to the single-porosity case with one additional term to account for the second fluid pressure. Applying this linear relation results in two coupled diffusion equations written in terms of the two pore pressures, independent of stress. A general analytical solution is given for matrix and fracture pressure histories and surface displacement.

(2) The constant stress and constant strain formulations are equally valid formulations, not competing theories. However, the negligible constant strain cross-storage coefficient assumption which has been invoked in the constant strain formulation leads to problems. Defining the fracture and matrix storage coefficients at a constant strain accentuates the problems. The constant stress formulation produces physically intuitive results for the column consolidation problem studied in this paper. The cross-storage, a_{23}, is small and indicative of the division of fluids in the two separate porosities.

(3) The double-porosity model produces fluid pressure and displacement histories at early times which cannot be adequately modeled using equivalent single-porosity assumptions. The magnitude of the differences between the single and double-porosity results is determined by the degree of interaction between the fracture and matrix.

Finally, the one-dimensional column consolidation boundary value problem provides a useful benchmark solution for the poroelastic behavior of a double-porosity continuum model. The direction of future work is to apply this model to other practical engineering and geophysical problems. For example, radial flow to a well, tidal loading, and earthquake loading in fractured-porous rocks are all problems where a poroelastic double-porosity model may provide additional insight.

Acknowledgement—This work was supported by the Department of Energy grant DE-FG-02-91ER14194.

REFERENCES

Bai, M., Elsworth, D. and Roegiers, J. C. (1993) Modeling of naturally fractured reservoirs using deformation dependent flow mechanism. *Int. J. Rock Mech. Miner. Sci. and Geomech. Abstr.* **30,** 1185–1191.

Barenblatt, G. I., Zheltov, I. P. and Kochina, I. N. (1960) Basic concepts in the theory of seepage of homogeneous liquids in fissured rocks. *Prikl. Mat. Mekh.* **24,** 852–864.

Berryman, J. G. and Wang, H. F. (1995) The elastic coefficients of double-porosity models for fluid transport in jointed rocks. *J. Geophys. Res.* **100,** 24,611–24,627.

Beskos, D. E. and Aifantis, E. C. (1986) On the theory of consolidation with double porosity. *International Journal of Engineering Science* **24,** 1697–1716.

Biot, M. A. (1941) General theory of three dimensional consolidation. *Journal of Applied Physics* **12,** 155–164.

Detournay, E. and Cheng, A. H. (1993) Fundamentals of poroelasticity. In *Comprehensive Rock Engineering*, ed. J. A. Hudson, Vol. 2, pp. 113–171. Pergamon Press.

Elsworth, D. and Bai, M. (1990) Continuum representation of coupled flow-deformation response of dual porosity media. In *Mechanics of Jointed and Faulted Rock*, ed. H. Rossmanith, pp. 681–688. Balkema.

Elsworth, D. and Bai, M. (1992) Flow-deformation response of dual-porosity media. *ASCE J. Geotech. Engrg* **118,** 107–124.

Goodman, R. E. (1980) *Introduction to Rock Mechanics*. John Wiley and Sons.

Hart, D. J. and Wang, H. F. (1995) Laboratory measurements of a complete set of poroelastic moduli for Berea sandstone and Indiana limestone. *J. Geophys. Res.* **100,** 17,741–17,751.

Khaled, M. Y., Beskos, D. E. and Aifantis, E. C. (1984) On the theory of consolidation with double porosity—III a finite element formulation. *Int. J. Num. Anal. Methods Geomech.* **8,** 101–123.

Terazghi, K. (1923) Die berechnung der durchlassigkeitsziffer des tones aus dem verlauf der hydrodynamischen spannungserscheinungen. *Sitzungsber. Akad. Wissen., Wien Math. Naturwiss. Kl., Abt. IIa* **132,** 105–124.

Tuncay, K. and Corapcioglu, M. Y. (1995) Effective stress principle for saturated fractured porous media. *Wat. Resour. Res.* **31,** 3103–3106.

Van der Kamp, G. and Gale, J. E. (1983) Theory of Earth tide and barometric effects in porous formations with compressible grains. *Wat. Resour. Res.* **19,** 538–544.

Wang, H. F. and Berryman, J. G. (1996) On constitutive equations and effective stress for deformable, double porosity media. *Wat. Resour. Res.* **32,** 3621–3622.

Warren, J. E. and Root, P. J. (1963) The behavior of naturally fractured reservoirs. *Soc. Pet. Eng. J.* **3,** 245–255.

Wilson, R. K. and Aifantis, E. C. (1982) On the theory of consolidation with double porosity. *International Journal of Engineering Science* **20,** 1009–1035.